A 10-bit 100-MS/s Reference-Free SAR ADC in 90 nm CMOS

Yan Zhu, *Student Member, IEEE*, Chi-Hang Chan, U-Fat Chio, *Student Member, IEEE*,
Sai-Weng Sin, *Member, IEEE*, Seng-Pan U, *Senior Member, IEEE*, Rui Paulo Martins, *Fellow, IEEE*, and
Franco Maloberti, *Fellow, IEEE*

Abstract—A 1.2 V 10-bit 100 MS/s Successive Approximation (SA) ADC is presented. The scheme achieves high-speed and low-power operation thanks to the reference-free technique that avoids the static power dissipation of an on-chip reference generator. Moreover, the use of a common-mode based charge recovery switching method reduces the switching energy and improves the conversion linearity. A variable self-timed loop optimizes the reset time of the preamplifier to improve the conversion speed. Measurement results on a 90 nm CMOS prototype operated at 1.2 V supply show 3 mW total power consumption with a peak SNDR of 56.6 dB and a FOM of 77 fJ/conv-step.

Index Terms—Charge-recovery, reference-free, switched technique.

I. INTRODUCTION

LOW POWER is the most relevant design concern for battery-powered mobile applications, such as DVB-T, DVB-H and TDMB [1]. Since the ADCs operate at tens of MS/s with 10 b to 12 b, the pipeline ADC is the commonly used architecture because of its power efficiency [2]–[4]. However, recently, the successive approximation register (SAR) architecture has re-emerged as a valuable alternative to the pipelined solution.

The conventional pipeline topology uses op-amps and switched capacitor structures to generate the residual. Moreover, the internal flash uses $2^n - 1$ comparators (n is the number of bits of the stage). All these blocks burn up power. Moreover, the reduction of supply voltage, as requested by sub-100 nm technologies, increases the consumed power because the reduced quantization step amplitude imposes an equivalent

increase of the transconductance. Recent works [5]–[9] optimize the power design of pipeline ADCs but the figure of merit (FoM) remains in the hundred of fJ/conv-step range.

The pipeline architecture does not benefit from the technology scaling because the use of low voltage supplies gives rise to an augmented consumption of power. In contrast, the scaling of technology does not penalize much the SAR ADC architecture because its analog part is simply made by a comparator and a capacitive DAC array. Indeed, the FoM values of state-of-art SAR ADCs [10]–[12] are well lower than those of pipelines and the best FoM in record is an SAR ADC [13]. The FoM of a SAR converter that improves with thinner line-widths is now in the range of tens of fJ/conv-step. However, for 65 and 90 nm technologies, the conversion rate is still low, not more than 50 MS/s.

The speed of a SAR ADC is determined by the time required by the DAC to settle within 1/2-LSB. With large number of bits and capacitive arrays, the main cause of power consumption is the reference generator that must provide very low output resistance. A second important source of consumed power is the dynamic power of the DAC. Previous works [12]–[14] improve the conversion efficiency by saving part of the switching energy during each bit cycling. However, the spared energy is a small fraction of the total power dissipated by the reference voltage generator, especially at high conversion speed [15]. Therefore, the power efficiency improves if the power needed by the reference generator is not accounted for [9], [16], [17]. When this power is included the FoM drops significantly.

This design obtains remarkable power effectiveness for medium resolution and high conversion speed by using two strategies: the first avoids the reference generator by directly using the supply voltages; the second saves the switching energy during the SA conversion. The use of the supply voltage as the reference of the ADC would lead to a signal swing of the converter that is wider than the typical signal range; this would reduce the effective SNR. This drawback is removed with the proposed technique that grants a passive gain by 2 of the input. A doubling of the LSB, that relaxes the limits of noise and offset, also lowers the power consumption of the comparator. In addition, it is worth to notice that a multiplication by 2 enables an input signal that is half the rail-to-rail and not the full rail-to-rail as is presented in [12], [13], [18], [19]. Having an input range of the converter well within the supply limit is suitable for signals generated on-chip. This is very common because the input of an ADC is the result of on-chip

Y. Zhu, C.-H. Chan, U.-F. Chio, S.-W. Sin and S.-P. U are with Analog and Mixed Signal VLSI Laboratory and Faculty of Science and Technology, University of Macau, Macao, China (e-mail: yanjulia@ieee.org; http://www.fst.umac.mo/en/lab/ans_vlsi/).

R. P. Martins is with Analog and Mixed Signal VLSI Laboratory and Faculty of Science and Technology, University of Macau, Macao, China. He is on leave from Instituto Superior Técnico/TU of Lisbon, Portugal (e-mail: RMartins@umac.mo).

F. Maloberti is with the Electronic Department, University of Pavia, Italy, and also with the University of Macau, Macao, China (e-mail: franco.maloberti@unipv.it)

Color versions of one or more of the figures in this paper are available online at http://ieeexplore.ieee.org.

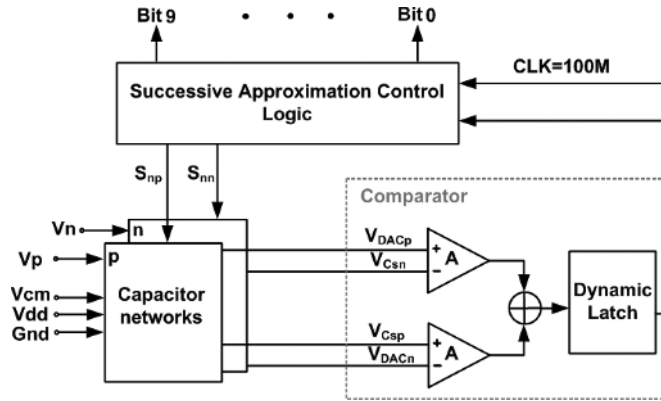Digital Object Identifier 10.1109/JSSC.2010.2048498

Fig. 1. Overall schematic diagram of the ADC architecture.

pre-conditioning, like amplification or filtering, obtained with op-amps whose signal swing represents headroom from the supply limits.

The switching energy saving technique, described in detail below, avoids the mismatch error at the conventional most significant bit (MSB) transition and enables a reduction by 2 of the overall capacitance used in the SAR. The charge recovery, implemented during each bit cycling, cuts by 1/3 the switching energy with respect to the one achieved in [12]. In addition, the used switching approach improves the conversion linearity that typically affects a conventional SAR ADC.

Instead of using the asynchronous processing [16] this paper avoids the fast clock by implementing a variable self-timed loop that adjusts the plus width of the preamplifier to reduce the ideal time for the LSBs conversions.

II. ADC ARCHITECTURE

Fig. 1 shows the architecture of the proposed 10-bit SAR ADC. It comprises differential capacitor networks, a dynamic comparator and the SA control logic. The differential capacitor networks are composed by 10-bit split schemes with the additional sampling capacitors C_s necessary for the passive multiplication by 2. The SA logic controls $V_{out,DAC} = V_{DACp} - V_{DACn}$ for bringing it toward $V_{out,Cs} = V_{Csn} - V_{Csp}$. In the comparator, the 4 inputs preamplifier and the dynamic latch determine the value of each bit. The SA control logic includes shift registers, bit registers and a switching logic block, which control the DAC operation to perform the binary-scaled feedback during the successive approximation cycle. The frequency of the clock used by the SA block is the ADC sampling frequency. No fast clock at the input is needed because the SA uses the self-timed technique. All the SA control signals result from a proper use of internal delay lines and their logic combination.

As mentioned in the introduction, the scheme presented in the next sub-section obtains as a great benefit the equivalent multiplication by two of the input. This permits the reference free operation and enhances the profit of charge recovery, thus reducing power consumption.
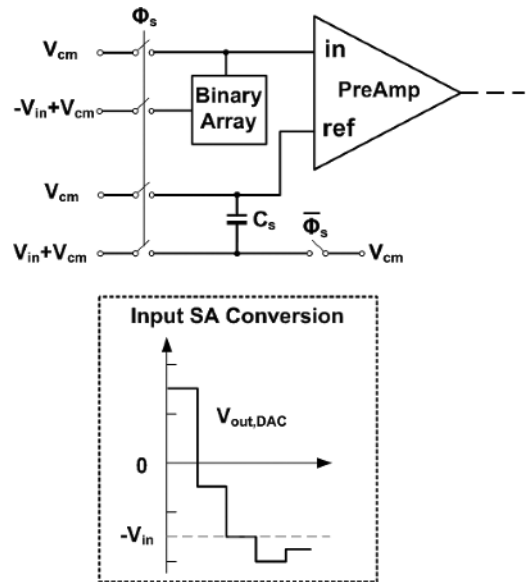

Fig. 2. Conceptual scheme that obtains a passive gain by 2.

A. Passive Multiplication by 2

A well-known feature of many SAR architectures is their insensitivity to parasitic capacitances. With conventional approaches the input of the comparator is at the reference voltage in the beginning of the conversion cycle and draws near the reference at the end of the conversion. As a result, the charge of the parasitic capacitance is almost the same at the beginning and the end of the conversion cycle. The schemes that are sensitive to parasitic experience a gain error and a linearity error. Obviously, the gain error due to the top-plate parasitic of DAC is not very important as it corresponds to an error of the voltage reference. More relevant is the non-linearity of the preamplifier input parasitic: the variation of the gate voltage may degrade the integral nonlinearity (INL). However, this parasitic nonlinearity effect is irrelevant: the parasitic of the preamplifier input is quite small when compared with the total capacitance of the DAC array. Therefore, the SAR ADC is, in practice, insensitive to the parasitic effects of both the DAC array and preamplifier. Consequently, for medium resolutions, parasitic insensitivity can be traded with other more valuable features. This design trades the parasitic insensitivity with the passive amplification by 2.

The conceptual scheme of Fig. 2 illustrates the method. During the sampling phase the binary-weighted capacitive DAC samples the input, like in a conventional scheme, while C_s samples the complementary input. During the conversion phase C_s shifts the voltage of the reference node to $-V_{in}$, making equal to $2V_{in}$ the signal that the SAR algorithm must compensate for.

The conventional SAR algorithm drives the DAC to finally converge to the common mode voltage (V_{cm}) at the end of the bit-cycling, according to

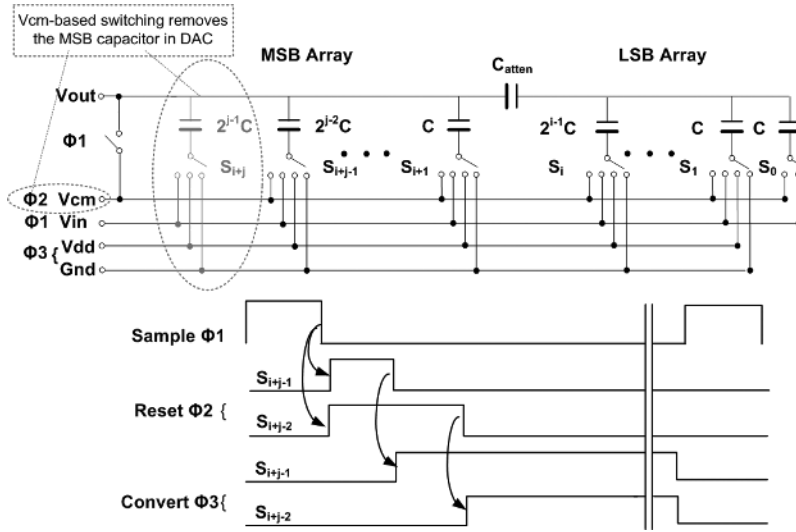$$V_{in} - \frac{\sum_n S_n C_n V_{ref,con}}{C_{DAC,Sum}} \to 0; \qquad (1)$$

Fig. 3. The V_{cm}-based switching timing diagram with its n-bit split capacitive DAC array (n = i + j).

on the contrary, the proposed method drives the DAC to converge toward $-V_{\text{in}}$ instead of V_{cm}

$$V_{\text{in}} - \frac{\sum_n S_n C_n V_{\text{ref,pro}}}{C_{\text{DAC,Sum}}} \to -V_{\text{in}} \qquad (2)$$

$$2V_{\text{in}} - \frac{\sum_n S_n C_n V_{\text{ref,pro}}}{C_{\text{DAC,Sum}}} \to 0 \Rightarrow V_{\text{ref,pro}} = 2V_{\text{ref,con}}. \qquad (3)$$

In the above equations S_n (1 or 0) is the ADC decision for bit n and C_n, $C_{\text{DAC,Sum}}$ represents the capacitors connected to the reference voltage $V_{\text{ref,con}}$ and the total array capacitance. Moreover, (3) certifies that the proposed operation corresponds to a passive amplification by 2 of the input. Furthermore, the proposed technique uses a reference voltage, $V_{\text{ref,pro}}$, that is twice $V_{\text{ref,con}}$, as used in the conventional counterpart. This is a key feature for the use of the supply voltage as reference. With $V_{\text{ref,pro}} = 1.2$ V identical to the supply voltage, the signal swing is 0.3–0.9 V with $V_{\text{cm}} = 0.6$ V, a value that allows the ADC to use signals generated by on-system stages biased by the supply voltage.

The sampling capacitor C_s serves to hold the input signal for the SA conversion, consequently no specific matching condition is required between C_s and the DAC array. However, C_s must be large enough to comply with the kT/C noise constraint.

In addition to the supply voltages this architecture uses the common mode voltage to pre-charge the capacitors. However, since the processing is fully-differential, no charge flows through the common mode terminal, unless there is a mismatch between the used common mode and the one of the input signal. Assuming that the mismatch is less than 10%, the common mode generator must provide a limited charge: 10 times smaller than what is required to references used in conventional SAR converters. Therefore, the output resistance of the common mode generator and its power needs are significantly relaxed.

B. V_{cm}-Based Switching Method

Switching the capacitive array consumes significant power. In order to reduce this term the value of the unit capacitance must be brought down to the limit allowed by the technology and the kT/C noise. Moreover, the use of the split capacitive array, that substitutes the full binary-weighted array, helps in the power reduction because the method reduces the total capacitance of the arrays. Further energy saving is obtained with effective switching approaches [12]–[14], [20], [21]. One of them, the set-and-down method recently proposed [12], saves significant switching energy thanks to its halving of the overall capacitance. The method used here, named V_{cm}-based switching approach, also obtains a half-capacitance reduction. In addition, as shown below, the switching sequence reduces the energy by an additional 1/3 with respect to the set-and-down technique.

The V_{cm}-based switching approach determines the sign of the differential input (MSB) by connecting the differential arrays to V_{cm}. The power dissipation is just derived from what is needed to drive the bottom-plate parasitic of the capacitive arrays, while in the conventional charge-redistribution [13], [22] and the charge-recycling [14] methods the necessary MSB "up" transition costs significant switching energy and settling time. Moreover, the MSB capacitor, being not required anymore, can be removed from the n-bit DAC array. Therefore, the next n − 1 bits estimation is done with an (n − 1) bit array instead of its n-bit counterpart, leading to half capacitance with respect to the conventional and charge-recycling methods.

Fig. 3 details the V_{cm}-based switching algorithm. In the global sampling phase Φ_1, V_{in} is stored in the capacitor array. During the resting phase Φ_2, all the capacitors' bottom-plates are switched to the common-mode voltage, resulting in the equivalent output voltage $-V_{\text{in}}$ at the output. The value of V_{out} determines the MSB during Φ_3 as the logic properly controls S_{i+j-1}. If $-V_{\text{in}} > 0$, S_{i+j-1} goes to G_{nd} while the other switches $S_{i+j-2,...}S_0$ remain connected to V_{cm}. The result is that the voltage at V_{out} [2] becomes $-V_{\text{in}} - V_{\text{ref}}/2$.
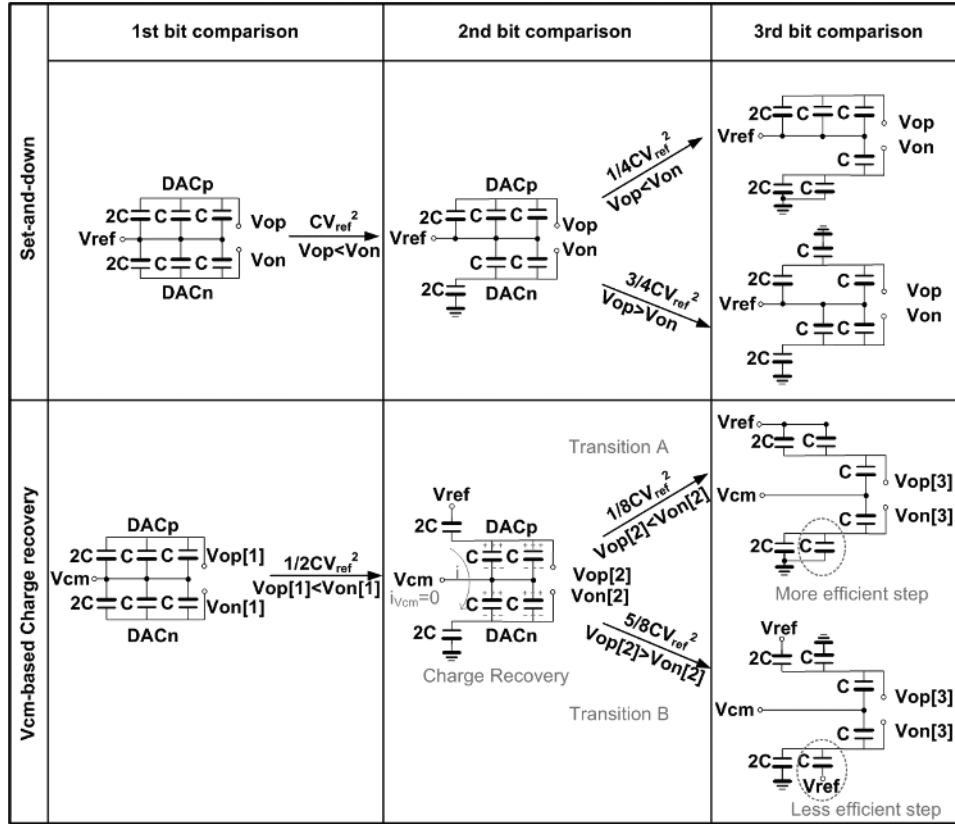
Fig. 4. A 3-bit example of set-and-down and proposed V_{cm}-based switching procedures.

If $-V_{in} < 0$, S_{i+j-1} is switched to V_{dd}, raising the voltage at $V_{out}[2]$ to $-V_{in} + V_{ref}/2$. The cycle is repeated for $n-2$ times.

The scheme of Fig. 3 and the above description are for a single ended operation. In reality, the fully differential operation makes the algorithm insensitive to the input common mode, $V_{cm,in}$. The difference between the common mode input and V_{cm} determines equal shifts $(V_{cm} - V_{cm,in})$ of the output of the array of Fig. 3. These shifts, assumed within the limits of the comparator common mode range, are rejected being a common mode component. Moreover, the V_{cm}-based switching method foresees "up" or "down" transitions after the comparator determines the bit and not before. This does not require pre-charging of capacitors and, possibly, their discharging after the bit decision. Therefore, the performed charge-redistribution is just what is required without wasting power. The only additional cost of this method is that it uses n more switches to initially reset all the capacitors to a common-mode voltage.

C. Charge-Recovery

The V_{cm}-based switching method operates in a similar way as the set-and-down [12] technique. Both reduce the capacitive array and simplify the MSB transition. However, for the determinations of the remaining $n-1$ bits there is a different switching sequence.

To outline the difference between the two methods Fig. 4 shows the operational steps of a 3-bit differential capacitive array performing the V_{cm}-based charge recovery and the

set-and-down methods. From [12] when the supply is directly used as the reference voltage, a rail-to-rail input signal is required. Fig. 4 illustrates the case where the input signal of the two methods is in both rail-to-rail. Accordingly, the reference voltage V_{ref} and the common-mode voltage V_{cm} in the two approaches are equal to V_{dd} and $1/2V_{dd}$, respectively. The switching energy needed for the first bit comparison is just what is necessary for driving the bottom-plate parasitics of the DAC arrays. Since the V_{cm}-based method charges the parasitic to half of the reference voltage, while the set-and-down uses the full reference, the consumed energy for the first bit comparison of the V_{cm}-based method is half of the set-and-down. The parasitic capacitance depends on technology and layout. Its value can be large because for medium and high-resolutions it is necessary to use electronic shielding on the top and the bottom which prevents couplings and noise injections.

The value of the MSB sets the arrays for second bit estimation. The SA logic controls the 2C of the DAC_p and DAC_n for "up" or "down" transition, respectively, as indicated also in Fig. 4, and the DACs' outputs finally settle to the following values:

$$V_{op}[1] = -V_{in} + V_{cm}$$
$$V_{on}[1] = V_{in} + V_{cm}$$
$$V_{op}[2] = -V_{in} + 3/4V_{ref}$$
$$V_{on}[2] = V_{in} + 1/4V_{ref}. \qquad (4)$$

The energy needed for the "up" transition in the DAC_p is E_up from $2C$ charged up from V_cm to V_ref and $E_{\text{Vcm,p}}$ from the other capacitors connected to V_cm. They are

$$E_\text{up} = -2CV_\text{ref}\left[(V_\text{op}[2] - V_\text{op}[1]) - (V_\text{ref} - V_\text{vcm})\right]$$
$$= 1/2CV_\text{ref}^2 \qquad (5)$$

$$E_{\text{Vcm,p}} = -2CV_\text{cm}(V_\text{op}[2] - V_\text{op}[1])$$
$$= -1/4CV_\text{ref}^2. \qquad (6)$$

For the "down" transition in DAC_n, the switching energy is only $E_{\text{Vcm,n}}$ coming from the capacitors connected to V_cm and the value is

$$E_{\text{Vcm,n}} = -2CV_\text{cm}(V_\text{on}[2] - V_\text{on}[1]) = 1/4CV_\text{ref}^2. \qquad (7)$$

From (6) and (7) it is deducted that the energy used by the differential DACs is complementary. Therefore, DAC_p compensates the energy drawn from V_cm by DAC_n. Qualitatively, the charge-recovery effect corresponds to a compensation of the charge transferred to DAC_n with charge coming from DAC_p, as illustrated also in Fig. 4. Accordingly, we don't need energy from V_cm in each bit-cycling. Due to the charge-recovery implementation, the "down" transition of DAC_n does not consume switching energy; the second bit comparison just needs the energy E_up for DAC_p where the capacitor $2C$ is charged from V_cm to V_ref. The switching energy of the second bit transition is output code independent, and it always obtains 50% less energy than the set-and-down which requires CV_ref^2 to discharge the same capacitor in one of the differential DAC arrays.

The estimation of the energy required for the 3rd bit estimation is code dependent and gives rise to the values indicated in Fig. 4. For the transition A the V_CM-based switching method is more advantageous; for the transition B the energy is almost the same.

For the conventional charge-redistribution method the switching energy also depends on the code. The consumed energy is much higher because of unnecessary charging and discharging actions. Fig. 5 compares the switching energy of the charge-recycling, the set-and-down and the V_CM-based approaches. The given figures assume equal unit capacitor for the 10 b capacitor arrays. For all the methods the peak of the consumed power occurs at half scale. The set-and-down method is more effective than the charge-recycling technique by almost a factor of 3. The V_CM-based switching method grants an additional 33% average benefit.

D. Linearity

As known the SAR algorithm does not ensure intrinsic monotonicity. The most critical transition for the conventional SAR ADC is at the middle range where half of the array switches-on and the other half (minus one) switches-off. The random variation ε_C of the value of the unity capacitance with variance σ_C renders rise to a differential nonlinearity (DNL) at the critical transistion equal to $\sqrt{2}\varepsilon_C \cdot 2^{N/2}$ [20], [23]. Since the V_CM-based switching approach determines
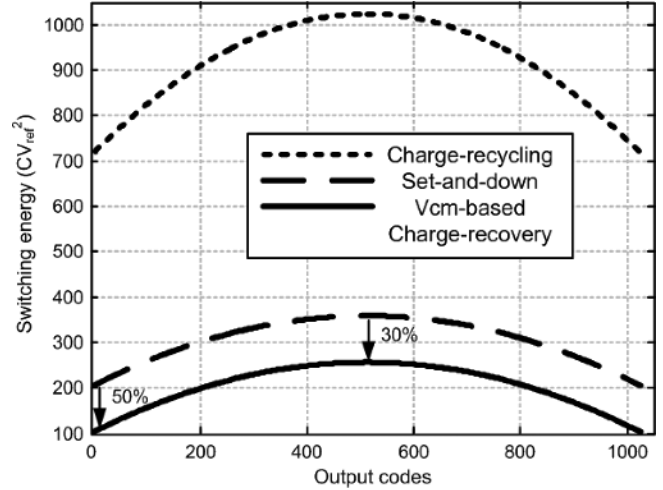

Fig. 5. Switching energy versus output code for three different techniques.

the MSB mismatch-independently, the worst case DNL occurs at $1/4V_\text{FS}$ and $3/4V_\text{FS}$. The feature relaxes the request of matching between unit capacitor by a factor $\sqrt{2}$. Therefore

$$\sqrt{2}\varepsilon_C \cdot 2^{(N-1)/2} < \frac{1}{2} \qquad (8)$$

that, for the used technology and 3σ design, gives $C_U > 12$ fF. However, this project employs a larger unity value: $C_U = 50$ fF. The choice serves to make negligible the effect of parasitic associated to the interconnection metal lines.

III. CIRCUIT DESIGN

A. Comparator Design

Fig. 6 shows the circuit schematic of the comparator with resistive loaded preamplifier and latch [24]. The comparator preamplifier has two differential pairs M1, M2 and M3, M4 connected to the outputs of the differential capacitive DAC and the additional sampling capacitor C_s. The currents at the output of the two pairs are summed up and injected on the resistive loads, R_d. The bias current and the load resistance yield a preamplifier gain of 27 dB.

The comparison cycling is divided into a reset phase and a regeneration phase. During the reset phase $(\text{STROBE} = 0)$, the preamplifier output is shorted to avoid memory effect of the comparison. Moreover, M11–M14 reset the regenerative loop and set the outputs V_op and V_on to V_dd. Since the current source transistor M15 is switched off no current flows from the supply to ground. When the regeneration phase starts $(\text{STROBE} = 1)$ M15 switches on and the input transistors M5–M6 force currents flowing through the back-to-back inverters M7–M8 and M9–M10 to amplify the voltage difference to a full swing.

The devices mismatch in the comparator bias does not affect the linearity of the conversion. Since the non constant common mode voltage is rejected by the CMRR of the preamplifier, the component mismatch gives rise to an equivalent input offset, as it is the case in conventional solutions.
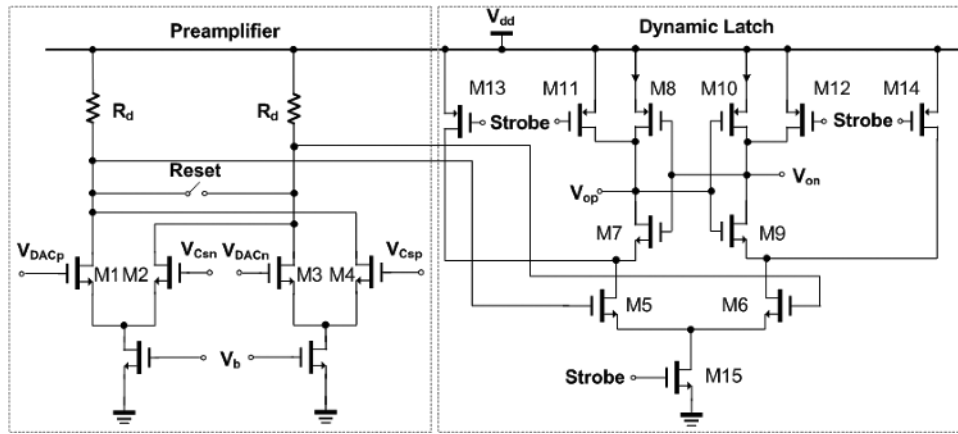
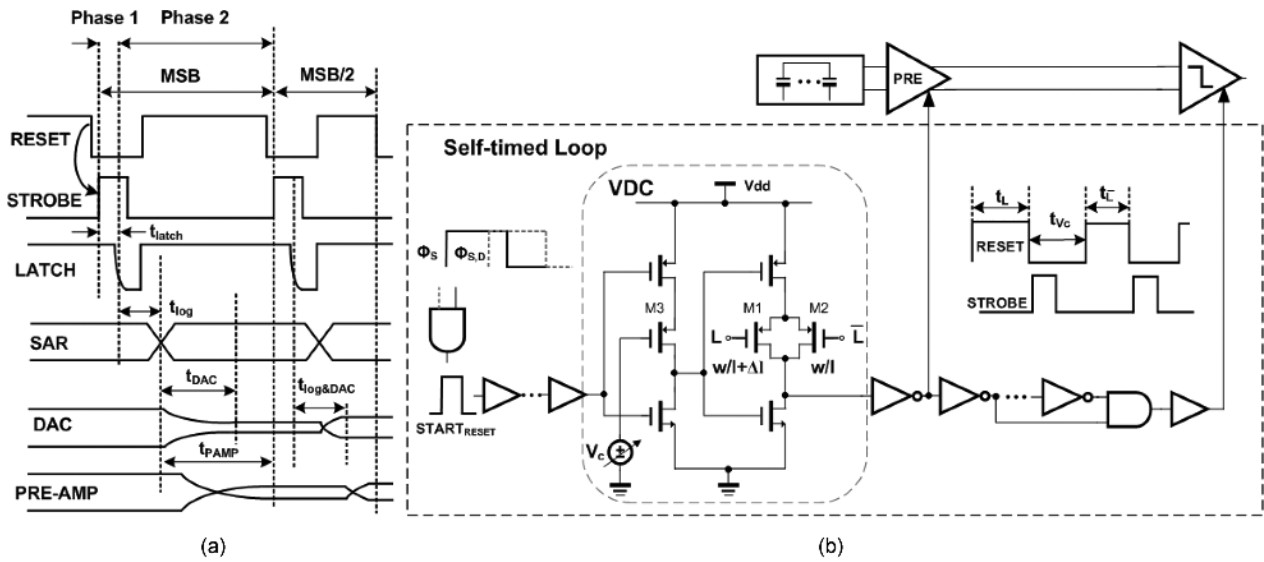Fig. 6.   Circuit schematic of the dynamic comparator.

Fig. 7.   (a) Timing diagram of bit-cycling. (b) Self-timed loop diagram and circuit schematic of VDC used to generate the preamplifier reset signal.

B. Variable Self-Timed Loop

The bit-cycling can be divided into two phases as shown in Fig. 7(a): phase 1 for regeneration of the latch that depends on the topology of the comparator; phase 2 for the SAR logic delay and settling for the DAC and preamplifier, which mainly depends on the DAC's structure and complexity of the logic. The asynchronous processing [16] can improve the conversion speed by synchronizing the bit-cycling with the latch's resolving time, which contributes with time saving between two adjacent strobes only when the time required by the phase 1 is significant. Furthermore, its implementation depends on the time required for phase 2 being identical and fast enough. Indeed, the ladder structure of the capacitive DAC [16] allows the bit switching of equivalent smaller capacitance instead of binary weighted capacitor array, thus insuring that the next comparison signal triggered by the previous output of the latch should start after the DAC and preamplifier are settled. However, in this design, the SA logic and DAC settling in phase 2 dominate the bit-cycling (i.e., the latch delay in phase 1 is much smaller). Since the MSBs are switched in the early

bit comparisons the conversion cycle is successively reduced according to the binary-weighted capacitor array. When the asynchronous processing is applied the comparison period will be always limited by the worst case DAC settling (the MSB/2 transition in this work), which loses the advantage of asynchronous operation. Instead, the scheme uses a variable delay controller (VDC) that optimizes the pre-amplifier reset signal according to the switching sequence. As shown in Fig. 7(b), the beginning of the reset signal is synchronous with the sampling clock Φ_S and its delayed $\Phi_{S,D}$ version, and it is triggered periodically by an inverter chain in series with the VDC. The pulsewidth of the reset signal is controlled by the different sized PMOS transistors M1 and M2, which are enabled or disabled according to the gate logic. The gate voltage of M3 is controlled by an external V_c to determine the tradeoffs between the extended settling time and ADC's performance.

C. SAR Logic

For high-speed operation the SAR logic must be minimized to achieve more spare time allocation for the DAC and preampli-
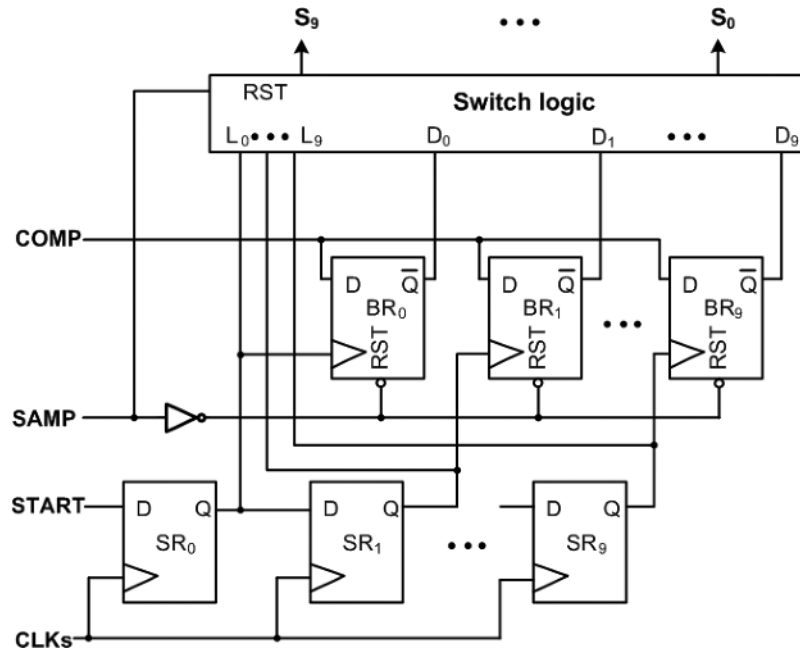
Fig. 8. Block diagram of the SAR logic.

fier settling. The SAR logic, shown in Fig. 8, consists of a set of shift registers [25] $(SR_0 - SR_9)$, bit registers [26] $(BR_0 - BR_9)$ and a switching logic block. The CLKs used to control the shift registers are synchronous with the reset of the comparator. The bit register detects each bit decision from the comparator and locks it for next stage processing. Since the circuit uses the V_{cm}-based switching the designed switching logic block obtains the outputs S_n according to the switching sequence of Fig. 3. Both the shift registers and bit registers are implemented in full custom dynamic logic, which provides a faster and lower power consumption SAR implementation.

D. Technology and Layout Considerations

The 10-bit SAR implementing the V_{cm}-based switching approach has been designed using a one-poly-nine-metal (1P9M) CMOS process with metal–insulator–metal (MIM) capacitor. The supply voltage is 1.2 V with a target conversion speed of 100 MS/s. The digital part of the SAR ADC obtains low power and fast conversion speed. Moreover, special care on the design of the layout prevents the capacitor mismatch and parasitic non-linearity effect [23].

Since the scheme uses the supply as reference, the switching speed of the capacitor array improves because the MOS transistors that realize the switches are controlled with a maximum overdrive. The split structure of the capacitive DAC requires a low parasitic in the array's LSB internal node [23]; furthermore, it is necessary to reduce the spur interference. The layout satisfies these two requests by using of MIM capacitors and a carefully layout routing. The result limits the top-plate parasitic to about 3%. As mentioned above, there is no requirement of matching between the capacitive DAC array and the sampling capacitor C_s. The only limitation is the kT/C limit that is very
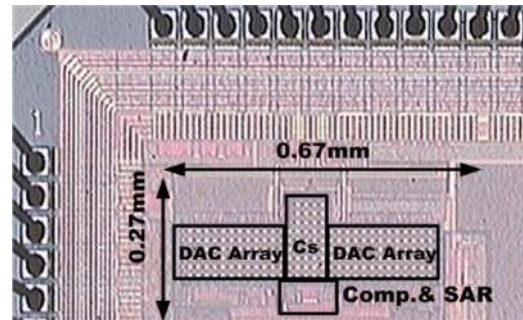

Fig. 9. Die microphotograph of the SAR ADC.

relaxed. The design uses $C_s = 8C_U$, where C_U is the unit capacitor equal to 50 fF. The split DAC leads to an architecture with 5 b MSB array and 4 b LSB array, being the total capacitance 2.75 pF.

IV. MEASUREMENT RESULTS

The prototype ADC was fabricated and tested. Fig. 9 shows the die photograph whose total active area is 0.18 mm^2. The ADC has a full-scale input range of $1.2V_{pp}$ differential, or $0.6V_{pp}$ single-ended. Fig. 10 shows the dynamic performance of the ADC with input frequency swept from 1.8 MHz to Nyquist. At a sampling rate of 100 MS/s the ADC can achieve 9.1 ENOB@1.8 MHz and 8.6 ENOB@Nyquist. Fig. 11 shows the ADC output spectrum with the input frequency at 1.8 MHz and 47 MHz. The second-harmonic distortion dominates the Spurious Free Dynamic Range (SFDR): 71 dB at low frequency and near Nyquist frequency 65 dB. The mismatch between two differential paths of the ADC is likely the cause. The third-harmonic becomes significant at Nyquist and the SNDR drops by 3 dB with a loss of 0.5 b. The distortion at high
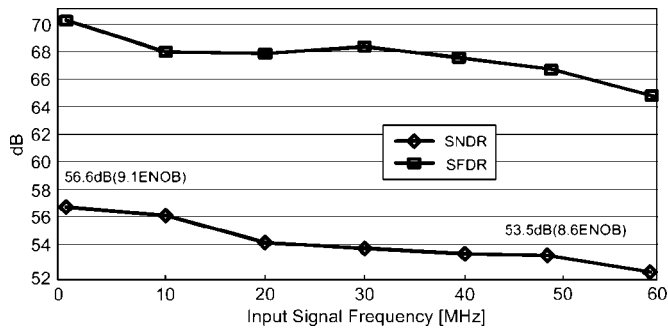
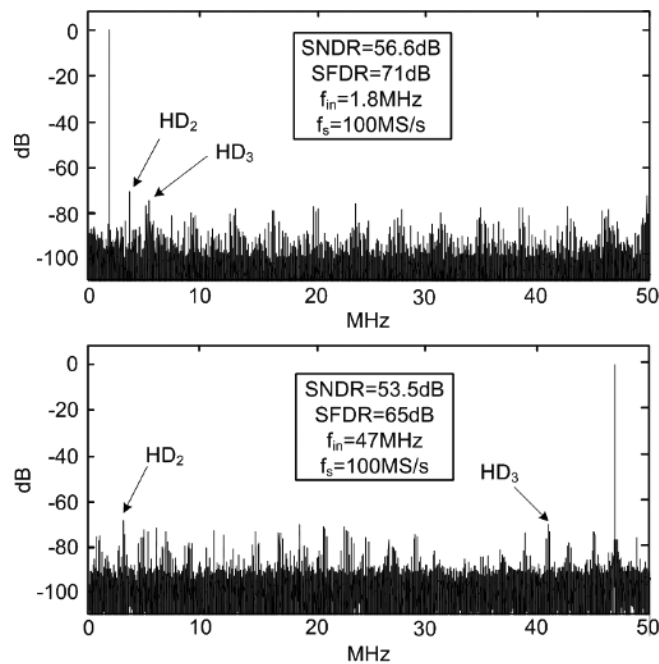Fig. 10.   Dynamic performance versus input frequency.

Fig. 11.   FFT of the digital output. The input is either a 1.8 MHz or a 47 MHz sine wave (full-scale) sampled at 100 MS/s.

Fig. 12.   Measured INL and DNL.

TABLE I
SUMMARY OF PERFORMANCE

Technology	90-nm CMOS
Resolution	10-bit
Sampling Rate	100-MS/s
Supply Voltage	1.2-V
Full Scale Analog Input	1.2-V_{PP} differential
SNDR	56.6dB
SFDR	71dB
ENOB	9.1-bit
FOM=Power/2^{ENOB}*f_s	55 fJ/conv-step
FOM=Power/2^{ENOB}*2*ERBW	77 fJ/conv-step
DNL	+0.79/-0.27LSB
INL	+0.86/-0.78LSB
Power Consumption	
Analog	1.3mW
Digital	1.7mW
Total	3mW

frequency increases because of a relatively high nonlinearity of the on-resistance of the sampling switches.

The DNL and INL are illustrated in Fig. 12. At 100 MS/s, the DNL and INL are $+0.79/-0.27$ LSB and $+0.86/-0.78$ LSB, respectively. Usually, the worst case DNL and INL happens in the middle (the MSB transition) in the conventional SAR ADC. The experimental measurements verify the benefit of the V_{cm}-based switching approach that imposes a lower DNL at the MSB transition. The INL is s-like and is minimized in the middle. The advantage is due to the MSB decision's independence of the capacitor mismatch as discussed in Section II-D. The worst cases DNL occur at points where the parasitic effect of the split DAC structure is more significant. The power consumption is 3 mW at 1.2 V. The analog power, including the capacitive DAC array, the comparator and the sampling network, is 1.3 mW and the digital power is 1.7 mW. Since the conventional tradeoff between conversion speed and power of the reference generator does not affect this design the digital power is a significant fraction of the total power dissipation. It is mainly drawn from the switches buffers and self-timed loop.
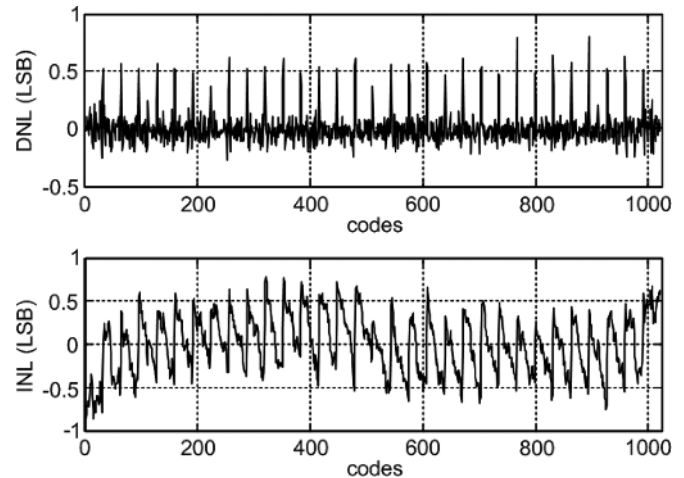
The measured performance of the prototype ADC is summarized in Table I. Table II compares this work with the state-of-the-art ADCs. The designs with a slightly better FoM [11], [12] are for lower speed and ENOB.

V. CONCLUSION

A 1.2 V 10-bit 100 MS/s SAR ADC has been presented. The reference-free and the power efficient V_{cm}-based switching technique enable high speed and low power SAR ADC's operation. The V_{cm}-based switching approach ensures a mismatch free MSB determination and, at the same time, saves capacitor area. The charge-recovery in each bit cycling leads to switching energy lower than both charge-recycling and set-and-down methods. The reference-free implementation and the passive multiplication by 2 avoid the use of the power-hungry resistive ladder/reference buffer without imposing a rail-to-rail input. The result is a fast *RC* settling and low power dissipation during SA conversion in the capacitive DAC array. The utilization

TABLE II
COMPARISON TO STATE-OF-THE-ART WORKS

	[9] ISSCC' 09	[27] VLSI' 08	[28] ISSCC' 08	[11] ISSCC' 08	[12] VLSI' 09	This work
Architecture	Pipelined	Pipelined	Pipelined	SAR	SAR	SAR
Technology	0.18-μm	90-nm	65-nm(with low V_t)	90-nm	0.13-μm	90-nm
Resolution	10-bit	9.4-bit	10-bit	9-bit	10-bit	10-bit
Sampling Rate	50-MS/s	50-MS/s	100-MS/s	40-MS/s	50-MS/s	100-MS/s
Supply Voltage	1.8-V	1.2-V	1.2-V	1-V	1.2-V	1.2-V
SNDR	58.2dB	49.4dB	59dB	53.3dB	52.8dB	56.6dB
ENOB	9.4-bit	7.91-bit	9.5-bit	8.6-bit	8.5-bit	9.1-bit
DNL	N/A	+0.37/-0.38LSB	+0.1/-0.1LSB	+0.7/-0.45LSB	+0.88/-1LSB	+0.79/-0.27LSB
INL	+0.7/-0.8LSB	+1.29/-0.88LSB	+0.2/-0.2LSB	+0.56/-0.65LSB	+2.2/-2.09LSB	+0.86/-0.78LSB
Power	9.9mW (P_{ref} not included)	1.44mW	4.5mW	820μW	920μW	3mW
FOM=Power/2^{ENOB}*f_s	300 fJ/step.	119 fJ/step.	62 fJ/step.	54 fJ/step.	52 fJ/step.	55 fJ/step.
FOM=Power/2^{ENOB}*2*f_{in}	337 fJ/step.	148 fJ/step.	62 fJ/step.	68 fJ/step.	64 fJ/step.	77 fJ/step.

of a variable self-timed loop minimizes the waste of time during each bit cycling and improves the conversion speed. The prototype ADC draws only 3 mW power from the 1.2 V supply and has a FoM of 77 fJ/step.

REFERENCES

[1] O. A. Adeniran *et al.*, "A CMOS low-power ADC for DVB-T and DVB-H systems," in *Proc. IEEE ISCAS*, May 2004, vol. 1, pp. 209–212.
[2] K. Honda *et al.*, "A low-power low-voltage 10-bit 100-M sample/s pipeline A/D converter using capacitance coupling techniques," *IEEE J. Solid-State Circuits*, vol. 42, no. 4, pp. 757–765, Apr. 2007.
[3] S.-T. Ryu *et al.*, "A 10-bit 50-MS/s pipelined ADC with opamp current reuse," *IEEE J. Solid-State Circuits*, vol. 42, no. 3, pp. 475–485, Mar. 2007.
[4] J. Li *et al.*, "A 1.8-V 22-mW 10-bit 30 MS/s pipelined CMOS ADC for low-power subsampling applications," *IEEE J. Solid-State Circuits*, vol. 43, no. 2, pp. 312–329, Feb. 2008.
[5] B. Murmann and B. Boser, "A 12 b 75 MS/s pipelined ADC using open-loop residue amplification," in *IEEE ISSCC Dig. Tech. Papers*, Feb. 2003, pp. 328–329.
[6] T. Sepke *et al.*, "Comparator-based switched-capacitor circuits for scaled CMOS technologies," in *IEEE ISSCC Dig. Tech. Papers*, Feb. 2006, pp. 220–221.
[7] S.-K. Shin and Sepke *et al.*, "A fully-differential zero-crossing-based 1.2 V 10 b 26 MS/s pipelined ADC in 65 nm CMOS," in *Symp. VLSI Circuits Dig. Tech. Papers*, Jun. 2008, pp. 218–219.
[8] M. Anthony *et al.*, "A process-scalable low-power charge-domain 13-bit pipeline ADC," in *Symp. VLSI Circuits Dig. Tech. Papers*, Jun. 2008, pp. 222–223.
[9] I. Ahmed *et al.*, "A 50 MS/s 9.9 mW pipeline ADC with 58 dB SNDR in 0.18 μm CMOS using capacitive charge-pumps," in *IEEE ISSCC Dig. Tech. Papers*, Feb. 2009, pp. 164–2165.
[10] J. Craninckx and G. V. Plas, "A 65 fJ/conversion-step 0-to-50 MS/s 0-to-0.7 mW 9 b charge-sharing SAR ADC in 90 nm digital CMOS," in *IEEE ISSCC Dig. Tech. Papers*, Feb. 2007, pp. 246–247.

[11] V. Giannini *et al.*, "An 820 μW 9 b 40 MS/s noise-tolerant dynamic-SAR ADC in 90 nm digital CMOS," in *IEEE ISSCC Dig. Tech. Papers*, Feb. 2008, pp. 238–239.
[12] C. C. Liu *et al.*, "A 0.92 mW 10-bit 50-MS/s SAR ADC in 0.13 μm CMOS process," in *Symp. VLSI Circuits Dig. Tech. Papers*, Jun. 2009, pp. 236–237.
[13] M. V. Elzakker *et al.*, "A 1.9 μW 4.4 fJ/conversion-step 10 b 1 MS/s charge-redistribution ADC," in *IEEE ISSCC Dig. Tech. Papers*, Feb. 2008, pp. 244–246.
[14] B. P. Ginsburg and A. P. Chandrakasan, "An energy-efficient charge recycling approach for a SAR converter with capacitive DAC," in *Proc. IEEE ISCAS*, May 2005, pp. 184–187.
[15] Z. Cao, S. Yan, and Y. Li, "A 32 mW 1.25 GS/s 6 b 2 b/step SAR ADC in 0.13 μm CMOS," in *IEEE ISSCC Dig. Tech. Papers*, Feb. 2008, pp. 542–543.
[16] M. S. W. Chen and R. W. Brodersen, "A 6 b 600 MS/s 5.3 mW asynchronous ADC in 0.13 μm CMOS," in *IEEE ISSCC Dig. Tech. Papers*, Feb. 2006, pp. 574–575.
[17] W. Liu *et al.*, "A 600 MS/s 30 mW 0.13 μm CMOS ADC array achieving over 60 dB SFDR with adaptive digital equalization," in *IEEE ISSCC Dig. Tech. Papers*, Feb. 2009, pp. 82–83.
[18] Y. F. Chen *et al.*, "Split capacitor DAC mismatch calibration in successive approximation ADC," in *Proc. IEEE CICC*, Sep. 2009, pp. 279–482.
[19] S.-K. Lee, S.-J. Park, and Y. Suh, "A 1.3 μW 0.6 V 8.7-ENOB successive approximation ADC in a 0.18 μm CMOS," in *Symp. VLSI Circuits Dig. Tech. Papers*, Jun. 2009, pp. 242–243.
[20] B. P. Ginsburg and A. P. Chandrakasan, "500-MS/s 5-bit ADC in 65-nm CMOS with split capacitor array DAC," *IEEE J. Solid-State Circuits*, vol. 42, no. 4, pp. 739–747, Apr. 2007.
[21] Y.-K. Chang *et al.*, "A 8-bit 500 KS/s low power SAR ADC for biomedical application," in *Procs. IEEE ASSCC*, Nov. 2008, pp. 228–231.
[22] A. Agnes *et al.*, "A 9.4-ENOB 1 V 3.8 μW 100 kS/s SAR ADC with time-domain comparator," in *IEEE ISSCC Dig. Tech. Papers*, Feb. 2008, pp. 246–247.
[23] Y. Zhu, U.-F. Chio, H.-G. Wei, S.-W. Sin, S.-P. U, and R. P. Martins, "A power-efficient capacitor structure for high-speed charge recycling SAR ADCs," in *Proc. IEEE ICECS*, Aug. 2008, pp. 642–645.
[24] V. Katyal, R. L. Geiger, and D. J. Chan, "A new high precision low offset dynamic comparator for high resolution high speed ADCs," in *Proc. IEEE APCCAS*, Dec. 2006, pp. 5–8.
[25] B. P. Ginsburg and A. P. Chandrakasan, "Dual time-interleaved successive approximation register ADCs for an ultra-wideband receiver," *IEEE J. Solid-State Circuits*, vol. 42, no. 2, pp. 247–257, Feb. 2007.

[26] U.-F. Chio, H.-G. Wei, Y. Zhu, S.-W. Sin, S.-P. U, and R. P. Martins, "A self-timing switch-driving register by precharge-evaluate logic for high-speed SAR ADCs," in *Proc. IEEE APCCAS*, Dec. 2008, pp. 1164–1167.

[27] J. Hu, N. Dolev, and B. Murmann, "A 9.4-bit, 50-MS/s, 1.44-mW pipelined ADC using dynamic residue amplification," in *Symp. VLSI Circuits Dig. Tech. Papers*, Jun. 2008, pp. 216–217.

[28] K. Honda, M. Furuta, and S. Kawahito, "A low-power low-voltage 10-bit 100-M sample/s pipeline A/D converter using capacitance coupling techniques," *IEEE J. Solid-State Circuits*, vol. 42, no. 4, pp. 757–765, Apr. 2007.
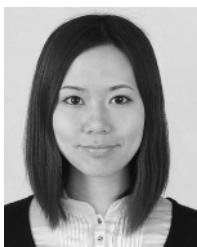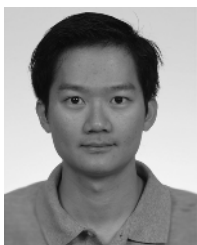
Yan Zhu (S'10) received the B.Sc. degree in electrical engineering and automation from Shanghai University, Shanghai, China, in 2006, and the M.Sc. degree in electrical and electronics engineering from the University of Macau, Macao SAR, China, in 2008. She is working in a research group of the Analog and Mixed-Signal VLSI Laboratory and pursuing the Ph.D. degree at the University of Macau.

Her research interests include low-power, high-speed monolithic A/D converter designs.

Chi-Hang Chan was born in Macau S.A.R., China, in 1985. He received the B.S. degree in electrical engineering from University of Washington, Seattle, in 2008. He is currently working toward the M.S. degree at University of Macau, Macao SAR, China.

His research interests include Nyquist ADC and mixed-signal circuits. Currently, his research mainly focuses on comparator offset calibration and ADC.

U-Fat Chio (S'07) received the B.Sc. degree in electrical engineering and the M.Sc. degree in communications engineering, both from National Sun Yat-Sen University, Taiwan, in 2002 and 2004, respectively.

From 2004 to 2005, he was with DenMOS Technology Inc., Hsinchu Science Park, Taiwan. Now he is studying in a research group of the Analog and Mixed-Signal VLSI Laboratory, University of Macau, Macao SAR, China. His research interest is high-speed analog and mixed-signal integrated circuit designs.

Sai-Weng Sin (S'98–M'06) received the B.Sc., M.Sc., and Ph.D. degrees with the highest honor in electrical and electronics engineering from University of Macau, Macao SAR, China, in 2001, 2003, and 2008, respectively.

He is currently an Assistant Professor in the Faculty of Science and Technology, University of Macau, and is the Coordinator of the Data Conversion and Signal Processing (DCSP) Research Line in Analog and Mixed-Signal VLSI Laboratory, University of Macau. His research interests include low-voltage, high-speed analog integrated circuit designs, high-performance data converters, as well as in the timing-jitter analysis and low-jitter clock generator designs for high-performance, high-speed mixed-signal systems. He has published over 30 technical journals and conference papers in the field of interests.

Dr. Sin is currently the Secretary of IEEE SSC Macau Chapter, and Treasurer/Secretary of IEEE CAS/COM Macau Joint Chapter and the Member of Executive Committee—Academic Affair of IEEE Macau, and has been a member of the Organization Committee of the 2004 IEEJ AVLSI Workshop, as well as the Special Session Co-Chair of the 2008 IEEE APCCAS Conference. He received the Chipidea Microelectronics Prize—Postgraduate Level in 2008 for outstanding academic and research achievements in microelectronics, as well as the Financial Support Award for the Student Paper Contest in ISCAS'05, and the Paper with Certificate of Merit for the RIUPEEEC'06.

Seng-Pan U (S'94–M'00–SM'05) received the B.Sc. and M.Sc. degrees in 1991 and 1997, respectively, and the joint Ph.D. degree from the University of Macau (UM) and the Instituto Superior Técnico de Lisboa in 2002 with highest honor in the field of high-speed analog IC design.

He has been with the Department of EEE/FST/UM since 1994. He is currently an Associate Professor. He co-founded in 2003 and is leading the Analog and Mixed-Signal VLSI research lab. Dr. U is also the advisor for more than 10 international student paper award recipients. He has published more than 100 scientific papers in IEEE/IET journals and conferences. He holds one U.S. patent (three filed) and has co-authored two scientific books at Springer. In 2001, Dr. U co-founded the Chipidea Microelectronics (Macau), Ltd.—the sole innovative-technology IC design company in Macau for devoting advanced analog and mixed-signal Semiconductor IP product development. He is currently the corporate Senior Analog Design Manager and Site Manager. (Chipidea was acquired in May 2009 by Synopsys Inc.).

Dr. U received the Excellent Young Scholar Award 2001 (1st Prize), The Most Favorite EEE Teacher Award 2002 and 2003, The FST Teaching Award 2004 from the UM. He also received The Young Researcher Award 2002 from Macau International Institute, and the National Lecture Fellowship 2005 from K. C. Wong Education Foundation for lectures in Tsinghua, Fudan and Zhejiang University. Dr. U is currently the Industrial Relationship Officer of IEEE Macau Section and the Chairman of IEEE Macau CAS/COMM and SSC chapters. He has been with technical review committee of various IEEE journals and conferences. He was the chairman of the local organization committee of IEEJ AVLSIWS'04, Technical Program co-Chair of IEEE APCCAS'08. He is also the Program Co-chair of ICICS'09 and Technical Program Committee of A-SSCC.

Rui Paulo Martins (M'88–SM'99–F'08) received the Bachelor, Masters, and Ph.D. degrees as well as the *Habilitation* for Full Professor in electrical engineering and computers from the Department of Electrical and Computer Engineering, Instituto Superior Técnico (IST), TU of Lisbon, Portugal, in 1980, 1985, 1992 and 2001, respectively.

He has been with the Department of Electrical and Computer Engineering/IST, TU of Lisbon, since October 1980. Since 1992, he has been on leave from IST, TU of Lisbon, and is also with the Department of Electrical and Electronics Engineering, Faculty of Science and Technology (FST), University of Macau (UM), Macao, China, where he is a Full Professor since 1998. In FST he was the Dean of the Faculty from 1994 to 1997 and he has been Vice-Rector of the University of Macau since 1997. From September 2008, after the reform of the UM Charter, he was nominated after open international recruitment as Vice-Rector (Research) until August 31, 2013. Within the scope of his teaching and research activity he has taught 20 bachelor and master courses and has supervised 21 Ph.D. and Masters theses. He has published 13 books, co-authoring three and co-editing ten, and five book chapters, 176 refereed papers in scientific journals and conference proceedings, as well as 70 other academic works, for a total of 264 publications, in the areas of microelectronics, electrical and electronics engineering, engineering and university education. He has co-authored seven submitted U.S. patents. He founded the Analog and Mixed-Signal VLSI Research Laboratory of UM: http://www.fst.umac.mo/en/lab/ans_vlsi/.

Prof. Rui Martins was the Founding Chairman of the IEEE Macau Section from 2003 to 2005, and of the IEEE Macau Joint Chapter on Circuits and Systems (CAS)/Communications (COM) from 2005 to 2008 [World Chapter of the Year 2009 of the IEEE Circuits And Systems Society (CASS)]. He was the General Chair of the 2008 IEEE Asia-Pacific Conference on Circuits and Systems (APCCAS'2008), and was elected Vice-President for Region 10 (Asia, Australia, the Pacific) of the IEEE Circuits and Systems Society (CASS), for the period 2009–2010. He is Associate Editor of the IEEE TRANSACTIONS ON CIRCUITS AND SYSTEMS PART II—EXPRESS BRIEFS for 2010–2011. He was the recipient of two government decorations: the Medal of Professional Merit from Macao Government (Portuguese Administration) in 1999, and the Honorary Title of Value from Macao SAR Government (Chinese Administration) in 2001.

Franco Maloberti (A'84–SM'97–F'96) received the Laurea degree in physics (*summa cum laude*) from the University of Parma, Parma, Italy, in 1968, and the Doctorate Honoris Causa in electronics from the Instituto Nacional de Astrofisica, Optica y Electronica (Inaoe), Puebla, Mexico, in 1996.

He was the TI/J.Kilby Chair Professor at the A&M University, Texas and the Distinguished Microelectronic Chair Professor at the University of Texas at Dallas. He was a Visiting Professor at The Swiss Federal Institute of Technology (ETH-PEL), Zurich, Switzerland and at the EPFL, Lausanne, Switzerland. Presently he is Microelectronics Professor and Head of the Micro Integrated Systems Group, University of Pavia, Italy and Honorary Professor, University of Macau, Macao SAR, China. His professional expertise is in the design, analysis, and characterization of integrated circuits and analog digital applications, mainly in the areas of switched-capacitor circuits, data converters, interfaces for telecommunication and sensor systems, and CAD for analog and mixed A/D design. He has written more than 400 published papers on journals or conference proceedings, four books, and holds 30 patents.

Dr. Maloberti was the recipient of the XII Pedriali Prize for his technical and scientific contributions to national industrial production, in 1992. He was co-recipient of the 1996 Fleming Premium, IEE, the Best Paper Award, ESSCIRC 2007, and the Best Paper Award, IEEJ Analog Workshop 2007. He received the 1999 IEEE CAS Society Meritorious Service Award, the 2000 IEEE CAS Society Golden Jubilee Medal, and the IEEE Millenium Medal. He was Vice President, Region 8, of the IEEE Circuit and Systems Society (1995–1997), Associate Editor of IEEE TRANSACTIONS ON CIRCUIT AND SYSTEMS PART II 1998 and 2006–2007, President of the IEEE Sensor Council (2002–2003), member of the BoG of the IEEE CAS Society (2003–2005) and Vice President, Publications, of the IEEE CAS Society (2007–2008). He is Distinguished Lecturer of the Solid-State Circuits Society.

Authorized licensed use limited to: UNIVERSITY OF PAVIA. Downloaded on June 29,2010 at 10:09:38 UTC from IEEE Xplore. Restrictions apply.